CHAPTER 2: MECHANISTIC STUDIES OF RUTHENIUM COMPLEX CELLULAR UPTAKE*

2.1: INTRODUCTION

Transition metal complexes have tremendous potential as diagnostic and therapeutic agents. They can be exploited for their modularity, reactivity, imaging capabilities, redox chemistry, and their precisely defined three-dimensional structure. An increasing number of biological applications have been explored.[1–3] Complexes that are currently in clinical use include the platinum anticancer drugs, radiodiagnostic agents containing ^{99m}Tc, and gadolinium(III) magnetic resonance imaging contrast agents.

In order to design new metal-based therapeutics more rationally, an understanding of the physiological processing of metal complexes is required. Though cellular uptake is critical to the success of a drug or probe, few mechanistic details are known regarding metal complex uptake. Different entry mechanisms may be preferred depending on the application, as the mode of entry affects cell-type specificity, the rate of internalization, and the fate of the compound once inside the cell. For example, entry by diffusion affords broad cell-type specificity, a great advantage in the use of fluorescent probes for live cell imaging. Conversely, medicinal chemists may seek to deliver drugs to target organs, taking advantage of tissue-specific transporters[4] or receptors.[5] For each mode of entry, there are also drawbacks. With protein-mediated transport, the degree of modification of

* Adapted from Puckett, C. A.; Barton, J. K. Mechanism of cellular uptake of a ruthenium polypyridyl complex. *Biochemistry* **2008,** *47,* 11711–11716.

the molecule is limited because transport relies on recognition. With endocytosis, molecules are often trapped in endosomes and face degradation by lysosomal enzymes.

Ruthenium(II) polypyridyl complexes are useful for studying cellular uptake due to their facile synthesis, stability in aqueous solution, and luminescence. Using confocal microscopy and flow cytometry, we have examined the uptake of a series of dipyridophenazine (dppz) complexes of ruthenium.[6] Despite its larger size, the lipophilic $Ru(DIP)_2dppz^{2+}$, illustrated in **Figure 2.1**, accumulates in cells more quickly than $Ru(bpy)_2dppz^{2+}$ (where bpy = 2,2′-bipyridine) and $Ru(phen)_2dppz^{2+}$ (where phen = 1,10-phenanthroline). $Ru(DIP)_2dppz^{2+}$ enters cells within an hour at micromolar concentrations, providing a reasonable time window for uptake experiments. Details of the cellular uptake mechanism of $Ru(DIP)_2dppz^{2+}$ can then be applied to understanding uptake characteristics of other structurally similar cationic metal complexes.

The biological activity of ruthenium complexes was first examined by Francis Dwyer in the 1950s, where a full family of tris(polypyridyl) complexes was shown to have bacteriostatic and anti-viral activities.[7] More recently, many ruthenium complexes have been tested for therapeutic potential,[8] and two ruthenium anticancer drugs (NAMI-A and KP1019) have reached clinical trials.[9,10] Cellular uptake of some ruthenium(III) complexes appears to be mediated by the iron transport protein transferrin. KP1019 (indazolium *trans*-[tetrachlorobis(1*H*-indazole)ruthenate(III)]) binds transferrin with displacement of a chloride ligand, and is transported into cells with transferrin by receptor-mediated endocytosis.[5] Ruthenium complexes lacking a labile ligand such as

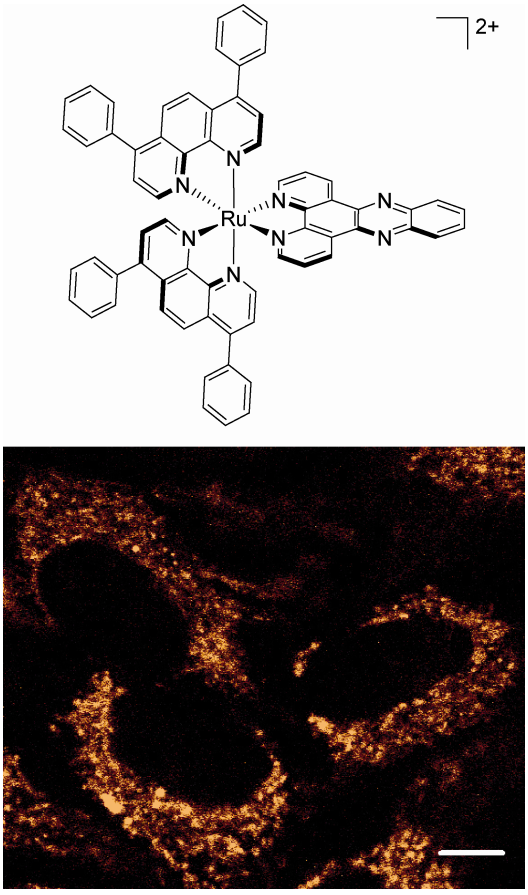

Figure 2.1: A luminescent ruthenium probe used to examine metal complex uptake. Top: Chemical structure of $Ru(DIP)_2dppz^{2+}$. Bottom: HeLa cells incubated with 5 μM $Ru(DIP)_2dppz^{2+}$ for 4 h, imaged by confocal microscopy. Note that the cytoplasm is extensively stained with the Ru complex. Scale bar is 10 μm.

chloride are unlikely to be able to enter cells in this manner and their mechanism of entry has not been established.

Such coordinatively saturated tris(chelate) ruthenium complexes furthermore serve as close fluorescent analogues of rhodium complexes that we have explored as potential chemotherapeutic agents.[11] These lipophilic, cationic rhodium complexes target single base mismatches in DNA and selectively inhibit cellular proliferation in mismatch repair-deficient cell lines.[3]

The main routes into a cell are endocytosis, active transport, facilitated diffusion, and passive diffusion. Due to its lipophilicity and positive charge, $Ru(DIP)_2dppz^{2+}$ likely traverses the membrane in response to the membrane potential, similar to other lipophilic cations such as tetraphenylphosphonium and rhodamine 123.[12,13] Here, we use chemical tools to elucidate the cellular uptake mechanism of $Ru(DIP)_2dppz^{2+}$, with the degree of uptake analyzed by flow cytometry.

2.2: EXPERIMENTAL PROTOCOLS

2.2.1.: MATERIALS

Cell culture reagents, transferrin-AlexaFluor488 conjugate, and TO-PRO®-3 were purchased from Invitrogen. Oligomycin, deoxyglucose, and the cation transporter inhibitors were obtained from Aldrich. Valinomycin was purchased from CalbioChem.

2.2.2: SYNTHESIS OF RU COMPLEXES

$Ru(DIP)_2dppz^{2+}$ and $Ru(phen)_2dppz^{2+}$ were synthesized as described previously (see also Chapter 1 of this text).[6] Briefly, $Ru(DIP)_2Cl_2$ and $Ru(phen)_2Cl_2$ were synthesized in an analogous fashion to $Ru(bpy)_2Cl_2$.[14] The dipyridophenazine (dppz) ligand was synthesized as previously described[15] and added to RuL_2Cl_2 by refluxing in ethanol-water for > 3 h to make $Ru(DIP)_2dppz^{2+}$ and $Ru(phen)_2dppz^{2+}$. The ethanol was removed by rotary evaporation, resulting in precipitation of $[Ru(DIP)_2dppz]Cl_2$, which was collected by filtration. $Ru(phen)_2dppz^{2+}$ was precipitated as the hexafluorophosphate salt, then returned to the chloride salt by Sephadex DEAE anion exchange column. The Ru complexes utilized are racemic mixtures of the two enantiomers.

2.2.3: CELL CULTURE

HeLa cells (ATCC, CCL-2) were maintained in minimal essential medium alpha with 10% fetal bovine serum, 100 units/mL penicillin, and 100 μg/mL streptomycin.

2.2.4: INDUCTIVELY COUPLED PLASMA MASS SPECTROMETRIC (ICP-MS) DETECTION OF RU

HeLa cells were grown to ~ 30% confluency in 75 cm^2 flasks and incubated with 5 μM $Ru(DIP)_2dppz^{2+}$ for 1 h at 37 °C in either medium with serum or medium without serum. The solution from the serum-free incubation was saved for circular dichroism measurements (described below). The cells were rinsed with PBS, detached with trypsin, and counted. The cells were isolated by centrifugation and digested in concentrated nitric

acid for 1.5 h at 60 °C. The solution was diluted with Millipore water to 2.0 mL for the incubation with serum and 20.0 mL for the serum-free incubation, adding nitric acid to give 2%. The Ru content was measured using a Hewlett Packard 4500 ICP-MS. Data are reported as the mean ± the standard deviation (n = 3).

2.2.5: ASSAY OF ENANTIOMERIC PREFERENCE IN RU UPTAKE

HeLa cells were grown to ~ 30% confluency in 75 cm^2 flasks and incubated with 5 μM $Ru(DIP)_2dppz^{2+}$ for 1 h at 37 °C in medium without serum and phenol red. After incubation, the medium was retrieved from the flask. The Ru complex was purified from the medium using a Waters C_{18} Sep-Pak. The solution was loaded onto a 1 g Sep-Pak equilibrated with water. The Sep-Pak was then rinsed with 150 mL water and 15 mL 20:80 $CH_3CN:H_2O$ with 0.1% TFA. The Ru complex was eluted with 90:10 $CH_3CN:H_2O$ with 0.1% TFA and lyophilized. For circular dichroism (CD) measurements, this isolated complex was dissolved in CH_3CN to give 8 μM complex. CD spectra were recorded on an AVIV 62 CD spectrometer.

2.2.6: METABOLIC INHIBITION

HeLa cells were detached from culture and treated with either 50 mM 2-deoxy-D-glucose and 5 μM oligomycin in PBS (to inhibit cellular metabolism) or 5 mM glucose in PBS for 1 h at 37 °C. Both solutions also contained 2.5 mg/mL bovine serum albumin fraction V (BSAV). The cells were then rinsed and suspended in either PBS with BSAV for the inhibition cells, or PBS with BSAV and 5 mM glucose for the control cells. The

cells were incubated with 10 mg/L transferrin-AlexaFluor488 or 5 μM $Ru(DIP)_2dppz^{2+}$ for 1 h at 37 °C. Following incubation, the transferrin-treated cells were rinsed with PBS and trypsinized to cleave the transferrin receptors from the cell surface.[16] The Ru-treated cells were rinsed. The cells were analyzed by flow cytometry. Ru-treated cells were not trypsinized following incubation, as rinsed cells and trypsinized cells gave the same mean luminescence in a control experiment: 282 ± 18 for the rinsed cells and 284 ± 23 for the trypsinized cells, following a 1 h incubation at 37 °C with 5 μM $Ru(DIP)_2dppz^{2+}$.

2.2.7: TEMPERATURE DEPENDENCE OF UPTAKE

HeLa cells were detached from culture and washed with Hanks' Balanced Salt Solution (HBSS) supplemented with 2.5 mg/mL BSAV. The cells were incubated with 5 μM $Ru(DIP)_2dppz^{2+}$ or $Ru(phen)_2dppz^{2+}$ for 2 h, or 10 mg/L transferrin-Alexa488 for 1 h, in HBSS with BSAV at 4 °C, ambient temperature (20–23 °C), or 37 °C. Transferrin-treated cells were trypsinized following incubation. The amount of uptake was analyzed by flow cytometry.

2.2.8: CATION TRANSPORTER INHIBITION

HeLa cells were detached from culture and washed with buffer (HBSS supplemented with BSAV), then pre-treated for 20 min with either 1 mM cation transporter inhibitor or buffer only. The cells were then incubated with 5 μM $Ru(DIP)_2dppz^{2+}$ for 1 h at ambient temperature. The cells were rinsed with buffer and Ru uptake was analyzed by flow cytometry.

2.2.9: MODULATION OF MEMBRANE POTENTIAL

HeLa cells were detached from culture and washed three times with either HBSS (containing 5.8 mM K^+) or high K^+-HBSS (containing 170 mM K^+), both supplemented with 2.5 mg/mL BSAV. Some of the cells in HBSS were pre-treated with 50 μM valinomycin for 30 min at 37 °C. The cells were incubated with 2 μM $Ru(DIP)_2dppz^{2+}$ for 1 h at 37 °C in one of the following solutions: HBSS, HBSS with valinomycin (to hyperpolarize the cells), or high K^+-HBSS (to depolarize the cells). The solutions also contained BSAV. After incubation, the cells were rinsed and the extent of uptake was analyzed by flow cytometry.

2.2.10: FLOW CYTOMETRY

Cells were detached from culture with EDTA (0.48 mM in PBS) and incubated at $1x10^6$ cells/mL with Ru complex (added from a concentrated DMSO stock) under conditions described above, then placed on ice. TO-PRO-3 was added at 1 μM immediately prior to flow cytometry analysis to stain dead cells. The fluorescence of ~ 20,000 cells was measured using a BD FACS Aria, exciting with the 488 nm laser for Ru and transferrin-AlexaFluor488, and with the 633 nm laser for TO-PRO-3. Emission was observed at 600–620 nm for Ru, 515–545 for AlexaFluor488, and 650–670 nm for TO-PRO-3. Cells exhibiting TO-PRO-3 fluorescence were excluded from the data analysis. Fluorescence data is reported as the mean ± the standard deviation (n = 3).

2.3: RESULTS

2.3.1: STRATEGY TO MEASURE UPTAKE

The dipyridophenazine (dppz) complexes of ruthenium serve as light switches for non-aqueous environments, luminescing only when bound to the hydrophobic regions of membranes, nucleic acids, and other macromolecules.[17,18] If the Ru complex decomposes or ligand substitution occurs, the resulting complex would no longer luminesce. Additionally the ligands themselves are not luminescent. Accordingly, the characteristic luminescence indicates that the complex inside the cell remains intact. We can use the luminescence of these ruthenium complexes to track their cellular uptake in both confocal microscopy and flow cytometry experiments. Confocal imaging confirms that $Ru(DIP)_2dppz^{2+}$ accumulates inside the cell rather than associating solely at the membrane surface, as seen in **Figure 2.1** and previously.[6] Ruthenium luminescence is observed throughout the cytoplasm, though mostly excluded from the nucleus. Flow cytometry, on the other hand, enables the rapid measurement of ruthenium luminescence intensity for multiple cell populations. Using primarily flow cytometry, we can then explore the cellular uptake mechanism of $Ru(DIP)_2dppz^{2+}$ by comparing the ruthenium luminescence following different incubation conditions.

2.3.2: ICP-MS MEASUREMENT OF RU UPTAKE

Inductively coupled plasma mass spectrometry (ICP-MS) measurements were performed to quantify the amount of Ru taken up by the cell. HeLa cells were treated with 5 μM $Ru(DIP)_2dppz^{2+}$ for 1 h at 37 °C in medium with or without serum. ICP-MS

measurements give 26.4 ± 6.3 amol of Ru per cell for the incubation in medium with serum, and 677 ± 73 amol per cell for the serum-free incubation. Assuming an average cell volume of 1.7 pL[19] and that the complex is evenly distributed throughout this volume, the Ru concentration in the cell is approximately 16 μM for incubation with serum and 398 μM for the serum-free incubation. These results indicate substantial concentration of the complex within the cell, with serum acting to attenuate the effective free ruthenium complex available in solution.

2.3.3: ENANTIOMERIC PREFERENCE IN UPTAKE

As racemic $Ru(DIP)_2dppz^{2+}$ was used for uptake experiments, we considered whether HeLa cells preferentially take in one enantiomer over the other. To test for enantioselectivity associated with uptake, we assayed for enantiomeric enrichment in the supernatant. Following incubation of 5 μM $Ru(DIP)_2dppz^{2+}$ with HeLa cells in serum-free medium, the Ru complex was recovered from the medium and the circular dichroism (CD) was examined. Serum-free medium was used for the incubation to remove any potential chiral bias created from interaction of the complex with serum proteins. ICP-MS determination of the Ru content of the cells confirms that a significant amount of Ru (~ 3% of the total) was taken in by the cells. Given this depletion, we estimate that an enantiomeric preference in uptake of 2.5:1 or greater would be detectable above instrument noise. However, the CD spectra of $Ru(DIP)_2dppz^{2+}$ after incubation with cells is within the level of the noise. This absence in optical activity indicates that any enantiomeric preference must be below this limit.

2.3.4: ENERGY-DEPENDENT UPTAKE MECHANISMS

Certain cellular uptake routes are energy-dependent, such as endocytosis[20] and active protein transport. These pathways are hindered when cells are incubated at low temperature (4 °C instead of 37 °C) or in ATP-depleted environments (e.g., from metabolic poisons). To determine whether $Ru(DIP)_2dppz^{2+}$ enters cells by an energy-dependent process, the complex was incubated with HeLa cells after ATP depletion by deoxyglucose (a glucose analogue that inhibits glycolysis) and oligomycin (an inhibitor of oxidative phosphorylation).[21, 22] As transferrin is internalized by clathrin-mediated endocytosis, fluorescently (AlexaFluor488) labeled transferrin was used as a positive control. The cellular uptake of $Ru(DIP)_2dppz^{2+}$ remains essentially unchanged when cells are under metabolic inhibition, with a mean luminescence of 659 ± 12 compared to 675 ± 10 for the cells not treated with deoxyglucose and oligomycin (**Figure 2.2**). Thus $Ru(DIP)_2dppz^{2+}$ appears to enter cells by an energy-independent process. In contrast, metabolic inhibition dramatically reduces the endocytosis of transferrin, demonstrated by the large decrease in the mean fluorescence from 3034 ± 52 to 210 ± 5.

The temperature dependence of $Ru(DIP)_2dppz^{2+}$ uptake was also explored. HeLa cells were incubated with the complex at 4 °C, ambient temperature (20–23 °C), and 37 °C (**Figure 2.3**). The mean Ru luminescence increases with incubation temperature, from 589 ± 17 at 4 °C to 826 ± 71 at 37 °C. Given the lipophilicity of $Ru(DIP)_2dppz^{2+}$, the increase in cellular uptake with temperature could also be the result of improved solubility in buffer at higher temperatures. To test this hypothesis, the temperature dependence of uptake was studied for a similar but more soluble complex,

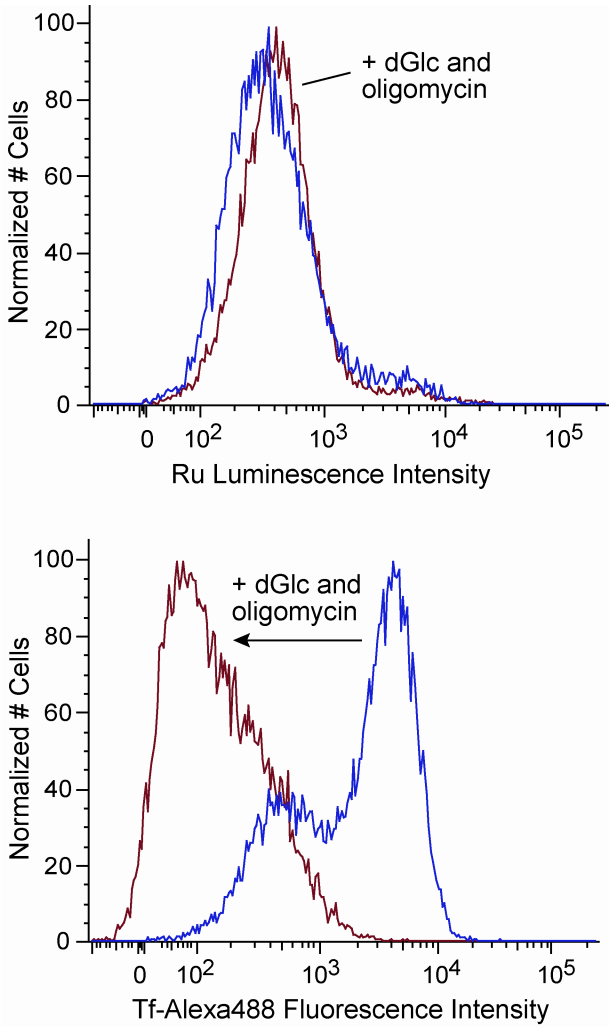

Figure 2.2: Flow cytometry measuring Ru incorporation used to examine the effect of metabolic inhibition on $Ru(DIP)_2dppz^{2+}$ cellular uptake. HeLa cells were pretreated for 1 h with 50 mM deoxyglucose (dGlc) and 5 μM oligomycin, then rinsed and incubated with 5 μM $Ru(DIP)_2dppz^{2+}$ or 10 mg/L transferrin-AlexaFluor488 (Tf-Alexa488) for 1 h. Cells treated with inhibitors (red) are compared to control cells (blue). Top: $Ru(DIP)_2dppz^{2+}$ uptake. Bottom: transferrin-AlexaFluor488 uptake.

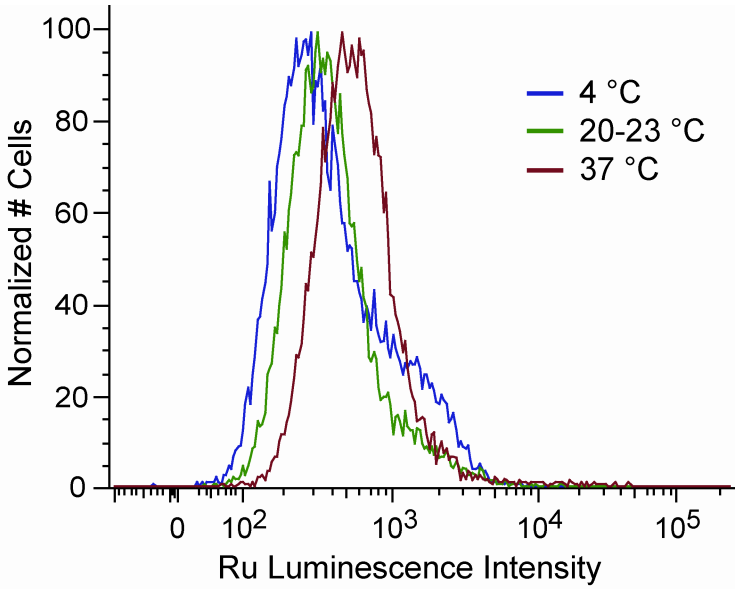

Figure 2.3: Effect of incubation temperature on $Ru(DIP)_2dppz^{2+}$ cellular uptake measured by flow cytometry. HeLa cells were incubated with 5 μM $Ru(DIP)_2dppz^{2+}$ for 2 h at 4 ºC, ambient temperature (20–23 ºC), or 37 ºC.

$Ru(phen)_2dppz^{2+}$. In this case, the mean luminescence remains roughly the same at the different incubation temperatures, 133 ± 10 at 4 °C and 141 ± 3 at 37 °C. Transferrin internalization was significantly more sensitive to temperature, with the mean fluorescence increasing from 480 ± 7 at 4 °C to 4071 ± 167 at 37 °C.

2.3.5: EFFECT OF ORGANIC CATION TRANSPORTER INHIBITORS

Organisms use polyspecific organic cation transporters (OCTs) for the distribution of endogenous organic cations and the absorption, distribution, and elimination of cationic drugs and toxins.[23] These transporters facilitate the diffusion of structurally diverse compounds. OCT substrates are typically organic cations and weak bases, though some neutral compounds and anions are also transported. Expression of the OCTs varies by tissue type. The carnitine and cation transporter OCTN2 has the most widespread tissue distribution among the OCTs, and its expression has been detected in some cancer cell lines, including HeLa.[24] Numerous compounds that inhibit OCT-mediated transport have been identified. Procainamide inhibits across the OCT family (including OCT1–3, OCTN1, and OCTN2). Tetraethylammonium ion is translocated by most of the OCTs, while other *n*-tetraalkylammonium salts inhibit OCT1 and OCT2, and for some OCTN1.[25]

To investigate whether $Ru(DIP)_2dppz^{2+}$ crosses the membrane using an organic cation transporter, uptake of $Ru(DIP)_2dppz^{2+}$ in the presence of OCT inhibitors was analyzed. HeLa cells were incubated with 1 mM inhibitor for 20 min before addition of $Ru(DIP)_2dppz^{2+}$ for 1 h. For OCTs, the IC_{50}s of the inhibitors used are generally less than

1 mM. Procainamide has an IC_{50} of < 3 mM and cimetidine <2 mM for OCTN2. As shown in **Figure 2.4**, the extent of uptake was analyzed by flow cytometry. Significantly, the *n*-tetraalkylammonium salts and procainamide do not appreciably alter the cellular uptake of $Ru(DIP)_2dppz^{2+}$. Within error, the cells have a similar mean luminescence intensity. The complex does not appear to use an organic cation transporter for entry into HeLa cells.

2.3.6: EFFECT OF MEMBRANE POTENTIAL

The plasma membranes of viable cells exhibit a membrane potential (−50 to −70 mV), with the inside of the cell negative with respect to the outside.[26] As $Ru(DIP)_2dppz^{2+}$ carries a positive charge, uptake may be driven by the potential difference across the cell membrane. The membrane potential in animal cells depends mainly on the K^+ concentration gradient. Here, the potential was reduced to close to zero by incubating the cells in buffer with potassium concentration equivalent to that found intracellularly (~170 mM).[27] This high potassium buffer (K^+-HBSS) was created by replacing sodium salts with equimolar potassium salts, while hyperpolarization of the membrane was achieved by adding valinomycin to low potassium buffer (HBSS).[28] Valinomycin is a cyclic peptide that selectively shuttles potassium ions across the membrane down the electrochemical potassium ion gradient, and it increases the membrane potential by exporting potassium from the cell.

$Ru(DIP)_2dppz^{2+}$ was incubated with HeLa cells for 1 h in either HBSS, HBSS with valinomycin (hyperpolarizes), or K^+-HBSS (depolarizes). The amount of Ru

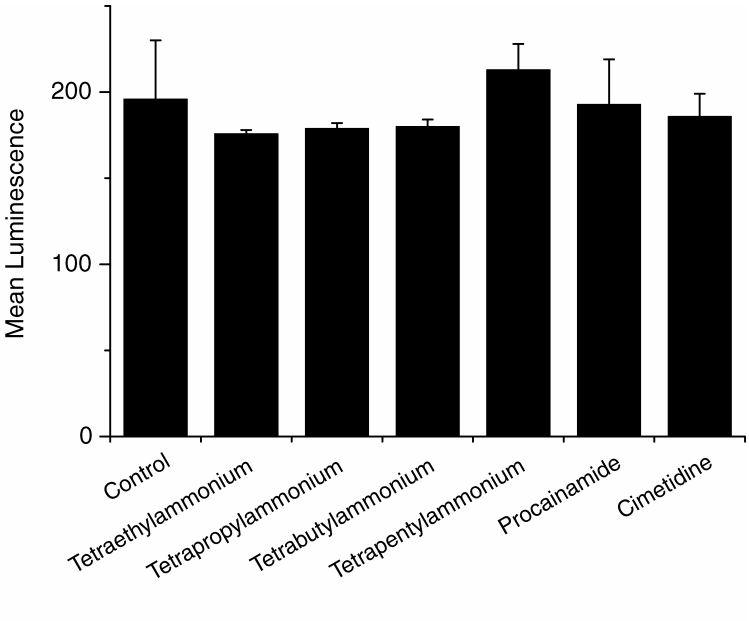

Figure 2.4: Effect of organic cation transporter inhibitors on $Ru(DIP)_2dppz^{2+}$ cellular uptake measured by flow cytometry. HeLa cells were pretreated with 1 mM inhibitor for 20 min, then 5 μM $Ru(DIP)_2dppz^{2+}$ was added for 1 h. Each data point is the mean ± the standard deviation of three samples.

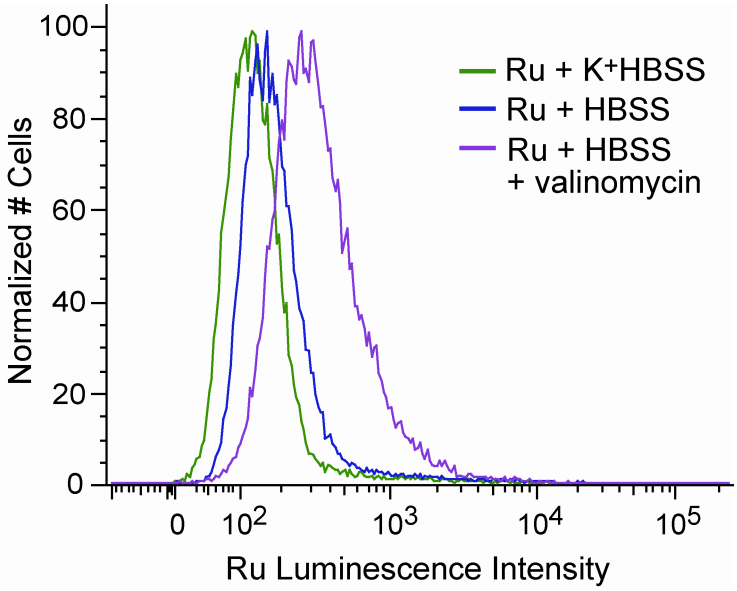

Figure 2.5: Effect of modulating the plasma membrane potential on $Ru(DIP)_2dppz^{2+}$ cellular uptake determined by flow cytometry. HeLa cells were incubated with 2 μM $Ru(DIP)_2dppz^{2+}$ in Hanks' Balanced Salt Solution (HBSS), HBSS with 50 μM valinomycin to hyperpolarize the cells, or modified HBSS with 170 mM potassium (K^+-HBSS) to depolarize the cells.

complex uptake was analyzed by flow cytometry (**Figure 2.5**). Depolarization of the plasma membrane reduces the uptake of $Ru(DIP)_2dppz^{2+}$, decreasing the mean luminescence of the cells from 232 ± 5 to 154 ± 1. Conversely, hyperpolarization of the membrane with valinomycin clearly promotes Ru complex uptake, increasing the mean luminescence to 428 ± 13. These results indicate that the positively charged complex is being driven inside the cells at least in part by the membrane potential.

2.4: DISCUSSION

Cellular uptake of small molecules can occur through energy-dependent (endocytosis, active transport) and energy-independent (facilitated diffusion, passive diffusion) processes. Metabolic inhibitors deplete the cell of energy, resulting in diminished uptake of molecules entering by endocytosis and active transport. HeLa cells treated with the metabolic inhibitors deoxyglucose and oligomycin show greatly reduced uptake (over 10-fold) of fluorescently labeled transferrin, which enters cells by endocytosis. On the other hand, deoxyglucose and oligomycin treatment cause no reduction of $Ru(DIP)_2dppz^{2+}$ cellular uptake, suggesting an energy-independent mode of entry. In fact, the midpoint of the luminescence intensity profile increases slightly in cells facing metabolic inhibition, though the mean fluorescence remains approximately the same. If $Ru(DIP)_2dppz^{2+}$ is actively exported, this efflux would be slowed under energy depletion and could explain the small increase. In contrast with the metabolic inhibition data, $Ru(DIP)_2dppz^{2+}$ uptake decreases slightly with lower temperature (4 °C versus 37 °C), consistent with energy-dependent transport. The difference is not as dramatic as

for transferrin, however, whose fluorescence changes 8-fold. Given that $Ru(DIP)_2dppz^{2+}$ is poorly soluble in buffer, this change may be due to improved solubility with temperature. Accordingly, a similar but more soluble complex, $Ru(phen)_2dppz^{2+}$, shows constant uptake at different temperatures. Low temperature also increases membrane viscosity, via decreased membrane fluidity, which can impair diffusion through the membrane.

The possible role of an organic cation transporter (OCT) in translocation of $Ru(DIP)_2dppz^{2+}$ across the membrane was also explored. These transporters facilitate the diffusion of endogenous organic cations as well as a variety of drugs and toxins. $Ru(DIP)_2dppz^{2+}$ uptake is not significantly altered in cells co-incubated with OCT inhibitors, indicating that the complex is likely not an OCT substrate. This result is consistent with the large size of $Ru(DIP)_2dppz^{2+}$ (~ 20 Å diameter) compared to known OCT substrates.

The cellular uptake of $Ru(DIP)_2dppz^{2+}$ is, however, influenced by the membrane potential. Consistent with diffusion of a positively charged molecule, uptake increases at higher potential and decreases at lower potential. That severe metabolic impairment does not discourage complex uptake is also consistent with diffusion. As both passage through a channel or passive carrier and diffusion directly through the lipid bilayer are energy-independent and respond to changes in the membrane potential, other factors must be considered to distinguish between these two mechanisms. The ability of $Ru(DIP)_2dppz^{2+}$ to enter the cell despite cation transporter inhibition, its larger size than typical

transporter substrates, and its relatively slow rate of cellular accumulation implicate passive diffusion as the mechanism of entry.

Passive diffusion is less cell-type specific, allows greater freedom for modification of the complex than transport via membrane proteins, and does not lead to entrapment in endosomes, as often occurs with endocytosis. As a result, this mechanism of passive diffusion may portend the broad applicability of metal complexes in different cell types for different intracellular functions. Certainly these results provide some basis for considering the biological activities that have already been identified for cationic transition metal complexes.[3,7] Significantly, knowledge of the mechanism of cellular uptake of this ruthenium(II) polypyridyl complex can now be applied to the design of structurally similar metal complexes for therapeutic and diagnostic use.

2.5: REFERENCES

1. Zhang, C. X.; Lippard, S. J. *Curr. Opin. Chem. Biol.* **2003***, 7,* 481–489.
2. Boerner, L. J. K.; Zaleski, J. M. *Curr. Opin. Chem. Biol.* **2005,** *9,* 135–144.
3 Hart, J. R.; Glebov, O.; Ernst, R. J.; Kirsch, I. R.; Barton, J. K. *Proc. Natl. Acad. Sci. U. S. A.* **2006,** *103*, 15359–15363.
4. Sai, Y.; Tsuji, A. *Drug Discovery Today* **2004,** *9,* 712–720.
5. Li, H.; Qian, Z. M. *Med. Res. Rev.* **2002,** *22,* 225–250.
6. Puckett, C. A.; Barton, J. K. *J. Am. Chem. Soc.* **2007***, 129*, 46–47.
7. Dwyer, F. P.; Gyarfas, E. C.; Rogers, W. P.; Koch, J. H. *Nature* **1952,** *170,* 190–191.
8. Clark, M. J. *Coord. Chem. Rev.* **2003,** *236,* 209–233.
9. Hartinger, C. G.; Zorbas-Seifried, S.; Jakupec, M. A.; Kynast, B.; Zorbas, H.; Keppler, B. K. *J. Inorg. Biochem.* **2006,** *100*, 891–904.
10. Bergamo, A.; Sava, G. *Dalton Trans.* **2007,** 1267–1272.
11. Zeglis, B. M; Pierre, V. C.; Barton, J. K. *Chem. Commun.* **2007,** 4565–4579.
12. Ross, M. F.; Kelso, G. F.; Blaikie, F. H.; James, A. M.; Cocheme, H. M.; Filipovska, A.; Da Ros, T.; Hurd, T. R.; Smith, R. A. J.; Murphy, M. P. *Biochemistry (Moscow)* **2005,** *70,* 222–230.
13. Davis, S.; Weiss, M. J.; Wong, J. R.; Lampidis, T. J.; Chen, L. B. *J. Biol. Chem.* **1985,** *260,* 13844–13850.
14. Sullivan, B. P.; Salmon, D. J.; Meyer, T. J. *Inorg. Chem.* **1978,** *17*, 3334–3341.
15. Dickeson, J. E.; Summers, L. A. *Aust. J. Chem.* **1970,** *23,* 1023–1027.

16. Bleil, J. D.; Bretscher, M. S. *EMBO J.* **1982,** *1,* 351–355.

17. Friedman, A. E.; Chambron, J.-C.; Sauvage, J.-P.; Turro, N. J.; Barton, J. K. *J. Am. Chem. Soc.* **1990,** *112,* 4960–4962.

18. Jenkins, Y.; Friedman, A. E.; Turro, N. J.; Barton, J. K. *Biochemistry* **1992,** *31,* 10809–10816.

19. Wheatley, D. N.; Inglis, M. S.; Foster, M. A.; Rimington, J. E. *J. Cell Sci.* **1987,** *88,* 13–23.

20. Schmid, S. L.; Carter, L. L. *J. Cell Biol.* **1990,** *111,* 2307–2318.

21. Barban, S.; Schulze, H. *J. Biol. Chem.* **1961**, *236,* 1887–1890.

22. Slater, E. C. *Methods Enzymol.* **1967**, *10,* 48–57.

23. Koepsell, H. *Trends Pharmacol. Sci.* **2004,** *25,* 375–381.

24. Wu, X.; Prasad, P. D.; Leibach, F. H.; Ganapathy, V. *Biochem. Biophys. Res. Commun.* **1998**, *246,* 589–595.

25. Koepsell, H.; Lips, K.; Volk, C. *Pharmacol. Res.* **2007**, *24,* 1227–1251.

26. Lodish, H.; Berk, A; Zipursky, S. L.; Matsudaira, P.; Baltimore, D.; Darnell, J. E. *Molecular Cell Biology,* 4th ed.; Tenney, S., Ed.; W. H. Freeman and Co.: New York, 2000.

27. Ehrenberg, B.; Montana, V.; Wei, M.-D.; Wuskell, J. P.; Loew, L. M. *Biophys. J.* **1988,** *53,* 785–794.

28. Shapiro, H. M. *Methods* **2000,** *21,* 271–279.